# Supporting Information

## Manu and Baccus 10.1073/pnas.1107994108

### SI Methods

**Multielectrode Recording.** Multielectrode array methods for extracellular recording, spike sorting, and analysis were as described (1). The salamander retina was isolated intact and then adhered by surface tension to a dialysis membrane attached to a plastic holder. It was then placed on a motorized manipulator and lowered onto a 60-electrode array (Multichannel Systems) ganglion cell side down. In this way, a large piece of retina, up to its entirety, could be placed on the array with minimal disturbance to the neural circuitry. The multielectrode array formed the bottom of a perfusion chamber, through which flows oxygenated Ringer solution buffered with bicarbonate. The full waveform of signals from the array of electrodes were digitized at 10 kHz and recorded to a computer.

**Intracellular Recording and Stimulation.** To allow for simultaneous intracellular recording with sharp electrodes, the electrode array chamber was mounted rigidly on a fixed stage that also held the intracellular electrode motorized manipulator. The retina was held in place over the electrode array under a ≈100-μm layer of 0.6% agarose, covered by a dialysis membrane containing several 100-μm holes. Extracellular electrodes were spaced 100 μm apart. The intracellular electrode was then guided under infrared light through a hole and the agarose layer to penetrate the retina from the photoreceptor side. Intracellular electrodes (150–250 MOhm impedance) were filled with 1–2 M potassium acetate. Current was injected into individual neurons by using custom software that commanded an intracellular amplifier operating in bridge mode. Current was timed with the visual stimulus to within 0.1 ms, allowing reproducible presentations of timed visual and current stimuli. The current amplitudes were chosen so they maintain the membrane potential within a physiological range given an estimate of the membrane conductance measured by using pulses of current. Injecting rapidly varying current through a sharp microelectrode prevents an accurate measurement of the membrane potential. Nonetheless, we can estimate the magnitude of membrane potential changes produced by using the measured membrane resistance of 40 ± 17 MΩ, and the measured membrane time constant of 17 ± 7 ms ($n$ = 6). Given the 0–50 Hz bandwidth of the current, we convolved the current with an exponential filter of the appropriate amplitude and estimated the resulting SD to be 9.6 ± 3.63 mV.

Results are included from 10 Off-type amacrine cells, which were identified by their light responses, the presence of an inhibitory surround, and their inhibitory transmission to Off-type ganglion cells with overlapping receptive field centers. Ganglion cells analyzed were biphasic Off-type cells classified with a uniform field visual stimulus (2).

**Record and Playback of Visual Responses.** To produce a timed perturbation of an amacrine cell's response, membrane potential fluctuations were first recorded from an amacrine cell for a given visual stimulus, $s(t)$, for 300 s. Then, the membrane time constant of the cell was measured by applying current pulses of 1 s. An exponential filter,

$$F_m = e^{-t/\tau}, \qquad \text{[S1]}$$

was fit to the voltage response with membrane time constant $\tau$. The recorded membrane potential fluctuations were then deconvolved by the exponential function. This created a current sequence, $I_a$ ($t$) that, when filtered through the membrane time constant according to

$$r(t) = \int F_m(t-\tau) I_a(\tau) d\tau, \qquad \text{[S2]}$$

matched the measured voltage response, $r(t)$. To amplify the cell's voltage fluctuations, the visual stimulus $s(t)$ was repeated for 300 s while injecting the current $I_a(t)$ synchronized with the visual stimulus so as to make both depolarizations and hyperpolarizations larger. The SD of the current was set to 500 pA. To diminish the cell's voltage fluctuations, $s(t)$ was repeated while injecting the current $-I_a$ ($t$), thus partially canceling the cell's visual input. This procedure allowed us to compare two opposite perturbations of the input. Note that this approach differs from voltage clamping to a fixed potential, in that it allows a cell's output to be amplified or diminished by a large or small amount. In addition, this approach differs from the dynamic clamp method (3) in that it requires no fast feedback response. Consequently, this approach can use a sharp microelectrode, allowing perturbation of an interneuron in the intact circuit without the need to slice the retina to perform patch recording on cells within the retina. Control, amplified, and diminished conditions were interleaved in intervals of 150 s.

***Visual stimuli.*** Stimuli were projected from a video monitor at a photopic mean intensity of ≈8 mW/m$^2$ and were drawn from a Gaussian distribution unless otherwise noted. Contrast defined as $W/M$ was 0.1–0.15, where $W$ is the SD and $M$ is the mean of the intensity distribution. Duration of stimuli was 300–900 s.

***Linear–nonlinear (LN) model of amacrine transmission.*** LN models of amacrine transmission were created using similar methods as has been described for visual stimuli (1). The stimulus $s(t)$ was white noise current with a bandwidth of 0–50 Hz and a 500 pA SD.

The current stimulus was convolved with a linear temporal filter, $F(t)$, which was computed as the time reverse of the spike triggered average stimulus, such that

$$g(t) = \int F(t-\tau) s(\tau) d\tau. \qquad \text{[S3]}$$

A static nonlinearity, $N(g)$, was computed by comparing all values of the firing rate, $r(t)$, with $g(t)$ and then computing the average value of $r(t)$ over bins of $g(t)$. The filter, $F(t)$, was normalized in amplitude such that it did not amplify the stimulus, i.e., the variance of $s$ and $g$ were equal (1). Thus, the linear filter contained only relative temporal sensitivity, and the nonlinearity represented the overall sensitivity of the transformation.

To compute the ganglion cell firing rate as a function of the predicted amacrine transmission (Fig. 4*D*), first the transmission filter $F_T(t)$ was computed by using white noise current injection. Then, a randomly flickering stimulus was presented without current injection to measure the amacrine cell membrane potential $V_a(t)$ and the ganglion cell firing rate $r(t)$. The predicted linear amacrine transmission $g_T(t)$ was computed by convolving $F_T(t)$ with $V_a(t)$, and then deconvolving by the amacrine cell membrane time constant. Finally, a nonlinear function mapping the predicted amacrine transmission to the ganglion cell firing rate was found by computing the average value of $r(t)$ over bins of $g_T(t)$.

Spatiotemporal receptive fields were measured by the standard method of reverse correlation (4, 5) of the firing rate or membrane potential response with a visual stimulus consisting of independently modulated 100-μm squares.

1. Baccus SA, Meister M (2002) Fast and slow contrast adaptation in retinal circuitry. *Neuron* 36:909–919.
2. Kastner DB, Baccus SA (2011) Coordinated dynamic encoding in the retina using opposing forms of plasticity. *Nat Neurosci* 14:1317–1322.
3. Prinz AA, Abbott LF, Marder E (2004) The dynamic clamp comes of age. *Trends Neurosci* 27:218–224.
4. Chichilnisky EJ (2001) A simple white noise analysis of neuronal light responses. *Network* 12:199–213.
5. Baccus SA, Olveczky BP, Manu M, Meister M (2008) A retinal circuit that computes object motion. *J Neurosci* 28:6807–6817.

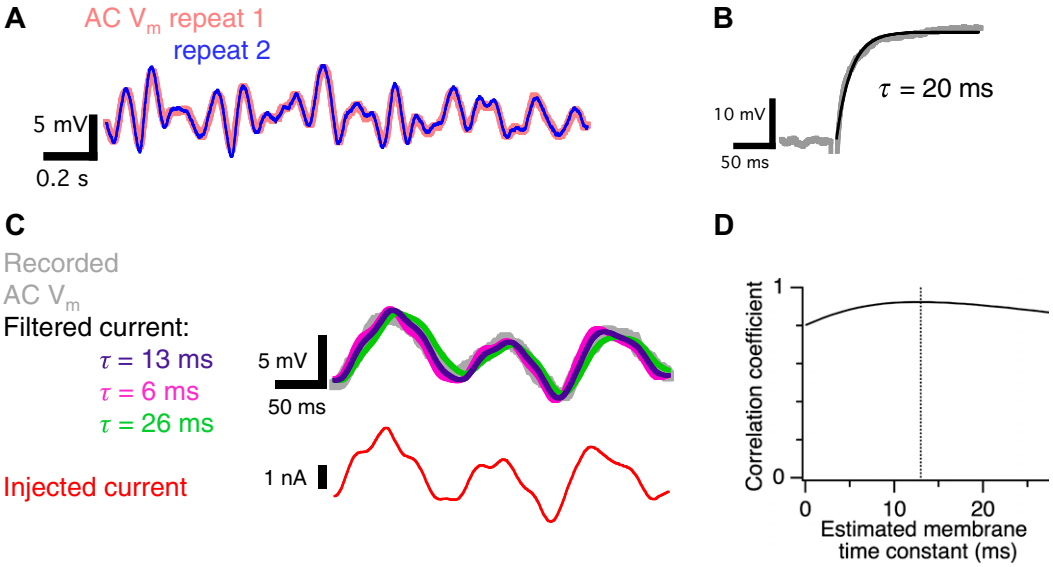


**Fig. S1.** Record and playback of amacrine visual response. (*A*) Membrane potential response of a sustained amacrine cell to two repeats of a uniform field random flicker stimulus. (*B*) Response to the offset of a −400 pA pulse injected into an amacrine cell. An exponential fit to the membrane time constant is shown. (*C*, *Upper*) Membrane potential response to the flickering visual stimulus compared with the current injected separately after it was filtered through exponential filters with three different membrane time constants. The actual membrane time constant was 13 ms. (*C*, *Lower*) The current injected into the cell. (*D*) For the cell in *A*, the correlation coefficient between the recorded membrane potential and the filtered current as a function of the estimated membrane time constant. If the estimate were incorrect, the correlation would decrease only slightly. Dotted line shows the actual membrane time constant of 13 ms.

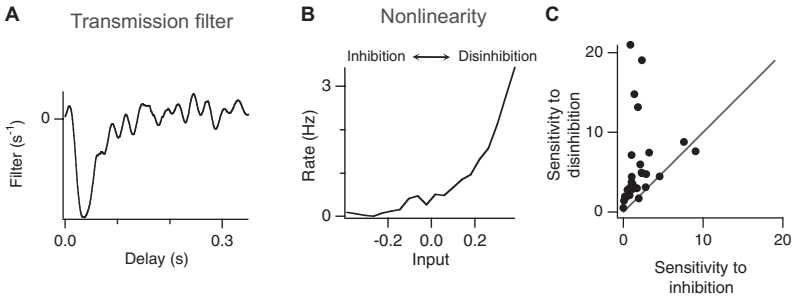


**Fig. S2.** Amacrine cell hyperpolarizations cause a greater change in ganglion cell firing than depolarizations. (*A* and *B*) Linear–nonlinear (LN) model between an amacrine and ganglion cell computed using white noise current injection as in Fig. 1. Stimulus duration was 300 s. (*A*) Linear transmission filter between the amacrine and ganglion cell. (*B*) Nonlinearity of transmission between the amacrine and ganglion cells. Zero input indicates the mean level of transmission. (*C*) The average slope of the nonlinearity above the mean level of transmission (sensitivity to disinhibition) compared with the average slope below the mean (sensitivity to inhibition).

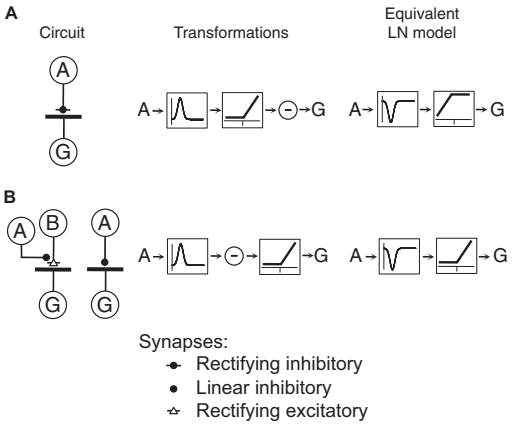


**Fig. S3.** LN models of different amacrine circuits. (*A*, *Left*) Circuit diagram showing amacrine transmission passing through a rectified inhibitory synapse. (*A*, *Center*) Sequence of transformations between the amacrine and ganglion cell, consisting of a temporal filter representing the filtering within the amacrine cell, followed by a threshold at the synapse and then a sign inversion at the postsynaptic receptor. (*A*, *Right*) The resulting LN model that would be computed across these transformations, consisting of a linear filter with a negative peak and a saturating nonlinearity. (*B*, *Left*) Circuit diagrams showing amacrine transmission passing through a linear inhibitory synapse either followed by a rectified excitatory synapse or directly onto a ganglion cell with a high spiking threshold. (*B*, *Center*) Sequence of transformations consisting of a temporal filter followed by a sign inversion at the postsynaptic receptor, and then a threshold from either the excitatory synapse or the ganglion cell. (*B*, *Right*) The resulting LN model that would be computed across these transformations, consisting of a linear filter with a negative peak and a threshold nonlinearity.